NRC Publications Archive
Archives des publications du CNRC

Numerical studies of the thermoelectrochemical performance of fuel cells
Beale, S. B.; Dong, W.; Zhubrin, S. V.

NRC Publications Record / Notice d'Archives des publications de CNRC:

National Research Council Canada   Conseil national de recherches Canada

Canada

Numerical Studies of the Thermoelectrochemical Performance of Fuel Cells

S.B. Beale W. Dong*

National Research Council, Ottawa
steven.beale@nrc.ca

S.V. Zhubrin

Concentration Heat and Momentum Ltd, London

ABSTRACT

The computer code PHOENICS was used to model transfer processes in solid oxide fuel cells. Detailed CFD models represent the best possible alternative to gathering experimental data. However for stacks of fuel cells the required computational meshes are very large. Therefore a simplified model based on a distributed resistance analogy was developed. The governing transport equations, together with associated calculations of heat generation, and electrochemistry are described. The models are then used to obtain data on the operation of solid oxide fuel cells. Results of calculations, in terms current density, cell voltage, species mass fractions and utilisation factors, are presented and discussed in detail together with suggestions for future work.

INTRODUCTION

Fuel cells produce electricity by the electrochemical conversion of gases with oxygen from air. The process is similar to that which takes place in a battery, except that a fuel cell is an open system, capable of producing electricity for as long as it is supplied with fuel and air.

The cell consists of two electrodes and an electrolyte. On one electrode a charged ion is produced, which is forced by the electrical field through the electrolyte to the other electrode. The ion reacts with the gas on the other electrode, provided there is an electron flow. This electron flow is generated at the first electrode and flows through an external circuit, generating an electrical current of the order of $10\,000$ A/m^2, at a voltage of 0.6 to 0.8 V. In this programme, attention is focussed on the Solid Oxide Fuel Cell (SOFC). This can utilise CO and CH$_4$ as well as H$_2$, as a fuel, and operates at a temperature of 700 to 800°C.
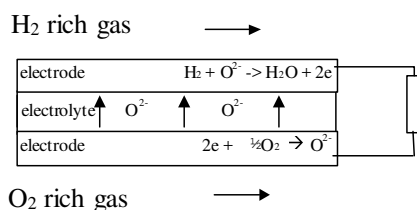

Figure 1. Main reactions in a SOFC.

The cell consists of a 1mm thick anode (the gas electrode), a 10μm thick electrolyte and a 50-100μm thick cathode (the air electrode). The electrolyte is as thin as practically possible to reduce ohmic losses. Figure 1 illustrates how the oxygen ion passes through the electrolyte and reacts with a gas molecule. Electrons flow through the external circuit, ensuring charge neutrality.

Cells are stacked by putting an interconnecting plate between each cell. This way cells are electrically connected in series and the flow of air and fuel to and from the cells is via manifolds. A dedicated system ensures that the gases are supplied at prescribed flow, temperature and pressure. The system also provides hydrogen for the fuel cell, by reforming methane or methanol in a reactor. Depending on the load, the electrical efficiency of a system running on natural gas can be over 50%. The remainder of the energy is released as heat, some of which is recovered.

Modelling of SOFC's can be traced to the early work of Archer (1962) and Sverdrup (1973). Since then, numerous fuel cell models have been developed and used for different types of fuel cells in different levels from macro-scale, cell-scale to micro-scale. Wepfer and Woolsey (1984) incorporated transport and kinetic

---

* Present address: Global Thermoelectric, Calgary, Alberta

properties to model irreversibility as voltage losses in an electrical network. Dunbar and Gaggioli (1990) conducted explicit modelling of transport and kinetic processes in SOFCs. Achenbach (1994) developed a 3-D stack model for SOFCs, including the kinetics of the reforming reaction. Bessette and Wepfer (1995) developed a model to evaluate the current flow distribution and irreversibility in a stack, with the thermal field evaluated using a simple conduction model. Foster (1999) employed a finite element analysis (FEA) package to calculate the flow field and the thermal field in a tubular SOFC. Yakabe (1999) developed a 3-D single-unit model to simulate the fluid flow, heat transfer, electric potential and current density, and also the internal stresses in a single-cell with double channels of co-flow and counter-flow. Ding (1997) and He (1998) developed a 3-D transient stack model for molten carbonate fuel cells using PHOENICS.

In this work, the focus is on developing a model with realistic electro-chemistry. Subsequently, simplified models are also described which can be used to describe large-scale stacks of fuel cells.

Basic model

The equations to be considered are the usual transport equations namely,

$$\frac{\partial(\rho\phi)}{\partial t} + \vec{\nabla}\cdot(\vec{u}\phi) = \vec{\nabla}\cdot\Gamma\vec{\nabla}\phi + S \qquad (1)$$

where ϕ takes the value 1 (continuity), $\vec{u}$ (momentum), y_i (mass fraction) and h (enthalpy), and Γ and S are diffusion coefficients and source terms, respectively. Fuel and air are treated as ideal gases. Reynolds numbers for both fuel and air are small, and a turbulence model was not therefore invoked. Solid and fluid physical properties are ennumerated at 700 °C.

At the anode surface, electrochemical oxidation takes place as:

$$H_2 + O^{2-} \rightarrow H_2O + 2e^- \qquad (2)$$

$$CO + O^{2-} \rightarrow CO_2 + 2e^- \qquad (3)$$
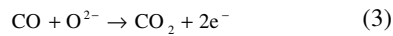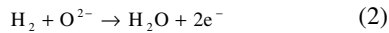
At the cathode surface, reduction takes place:

$$O_2 + 4e^- \rightarrow 2O^{2-} \qquad (4)$$

The surface rates, J, for H_2, H_2O and O_2 can be related to local current density, i, by Faraday's law
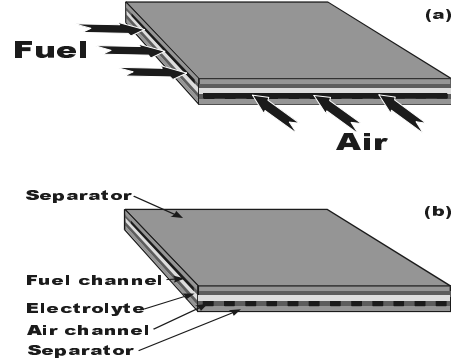
Figure 2 The geometry of simulated single cell-unit

$$J = -\frac{M}{1000}\frac{i}{\nu\,F} \qquad (5)$$

where M is molecular weight, ν is valence, and F is Faraday's constant. The cell voltage, V, can be computed as

$$V = E - iR_i - \eta_a - \eta_c = E - ir_i \qquad (6)$$

where η_a and η_c are anodic and cathodic overpotentials. $R_i\,(\Omega m^2)$ is the local Ohmic resistance, $r_i\,(\Omega m^2)$ can be regarded as a locally 'lumped internal resistance' of the cell, E is the Nernst potential;

$$E = E^0 + \frac{RT}{2F}\ln\left(\frac{x_{H_2}x_{O_2}^{0.5}}{x_{H_2O}}\right) + \frac{RT}{4F}\ln P_a \qquad (7)$$

where x_i are mole fractions (mol/mol), and P_a is local air pressure.

The heat source due to the electrothermal effect of Ohmic resistance and overpotentials can be expressed as

$$\dot{q}_e = \frac{i(E-V)}{L_{cell}} \qquad (8)$$

where L_{cell} is the thickness of the cell sheet. A fourth-order least-squares polynomial fit to experimental data (Ghosh et al., 2001) valid in the range 550 to 1200 °C, was used to compute the Ohmic resistance and electrolyte overpotentials in Eq. (6).

The geometry is such that a Cartesian mesh, passing through both solid and fluid zones, was conveniently employed. Figure 2 The geometry of simulated single cell-unit. The main components of the cell are the top separator, fuel channel, electrolyte and electrodes, air channel, and bottom separator. Fuel and air are in

cross-flow. Two designs were considered: (a) with both the fuel and air channels in the form of flat rectangular ducts, (b) with numerous individual air channels and a single rectangular fuel channel, as shown.

The calculation proceeds as follows: (1) Initial values are assumed for transport properties, cell voltage V etc. (2) The main calculation procedure is commenced and heat and mass source terms computed. The transport equations, Eq. (1), are solved. (3) The open circuit voltage and internal resistance are then computed, and the local current density obtained. Steps (2) and (3) are repeated until sufficient convergence is obtained. The basic model was used to calculate performance in single-cells and in stacks of cells.

Either the cell voltage or the overall current (or average current density) require to be prescribed. For the latter case 'voltage correction' is applied in a suitably simple manner, based on the average value of $\partial E/\partial i$ obtained in the usual manner, by differentiating Eq. (6).

$$V' = -R\bar{i}' \tag{9}$$

$V = V^* + V'$ where V^* is the value of V at the previous sweep, and similarly $\bar{i}' = \bar{i} - \bar{i}^*$. Thus the mean current density, $\bar{i}^*$, is computed in GROUND at the end of each of sweep compared to the desired value, $\bar{i}$ and the voltage corrected accordingly, R is a measure of the resistance of the cell, the exact value of which is not important; convergence is readily obtained with any reasonable R-value.

Stack model

Because detailed numerical simulations require very large meshes, alternative methodologies were devised for stack modelling. The method is a modified version of the distributed resistance analogy of Patankar and Spalding (1972). Beale et al. (2000) employed this methodology considering the flow of a single phase (only) in the manifolds and passages of a SOFC in the absence of heat and mass transfer. Here simultaneous flow of both working fluids with the associated coupled heat/mass transfer is computed using local volume averaging so that,

$$\text{div}(r\rho\vec{u})_k = S_k \tag{10}$$

$$\text{div}(\rho r\vec{u}; \vec{u})_k = -r_k \,\text{grad}\, p_k + \text{div}\, r_k \mu \,\text{grad}\, \vec{u}_k + F_k r_k^2 \vec{u}_k \tag{11}$$

$$\text{div}(r\rho\vec{u}\phi)_k = \text{div}\, r_k \Gamma \,\text{grad}\, \phi_k + S_k + \alpha_{jk}(\phi_j - \phi_k) \tag{12}$$
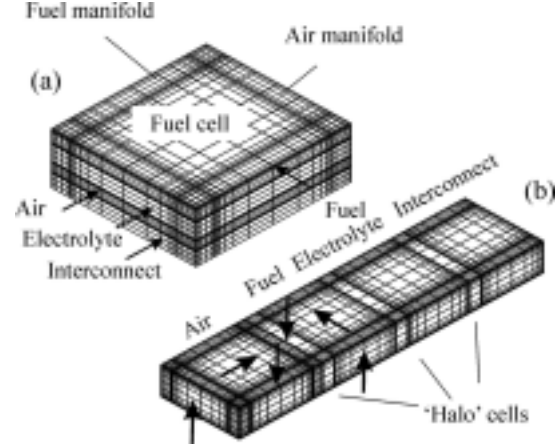

Figure 3 Meshes used in this study (a) Detailed model of single cell (b) MUSES distributed resistance analogy approach.

where $k = a$ (air), f (fuel), e, (electrolyte), or i, (interconnect), as appropriate. The temperature distribution in the electrolyte is also solved in the usual fashion. Because local volume averaging is employed, there are now two velocities and pressures corresponding to the air and fuel, in each computational cell, and temperatures in all fluid and solid zones. The chosen solution was to implement the multiply-shared space (MUSES) method in PLANT. The main ideas are to provide as many blocks of grid as necessary to cover the same volume of space in question and on each of these to solve for a different variable: (1) air; (2) fuel, (3) electrolyte, etc. Since values of variables (such as temperature) on any one grid may depend on those in another grid; these inter-phase terms are taken as sources.

The viscous term is replaced by a resistance or drag distributed throughout the volume of the device. In the scalar equations, the diffusion term is supplanted by an inter-phase terms α_{jk} are 'volumetric heat/mass transfer' coefficients. Thus the distributed resistance method replaces diffusive effects with a rate equation, however inertial effects are still accounted for. It thus represents a model intermediate between direct numerical calculations and classical heat/mass transfer methods. Time prevented stack models using either detailed CFD calculations or the MUSES approach from being conducted for variable local current density. These calulations presume both the current density and the Ohmic resistance of the electrolyte to be constant.
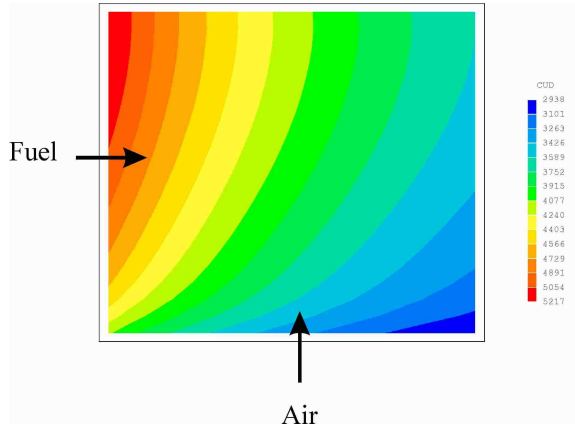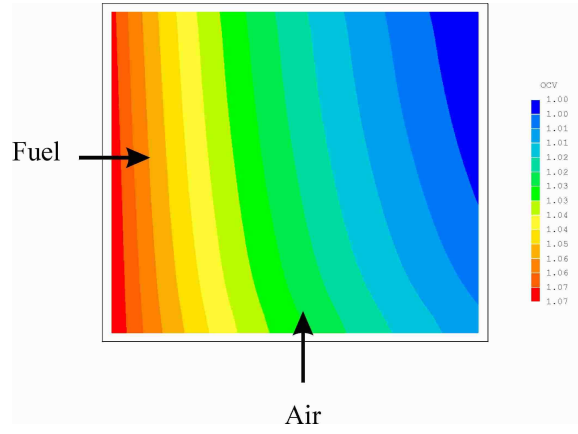
Figure 4. Current density, $\bar{i}$ = 4 000 A/m^2

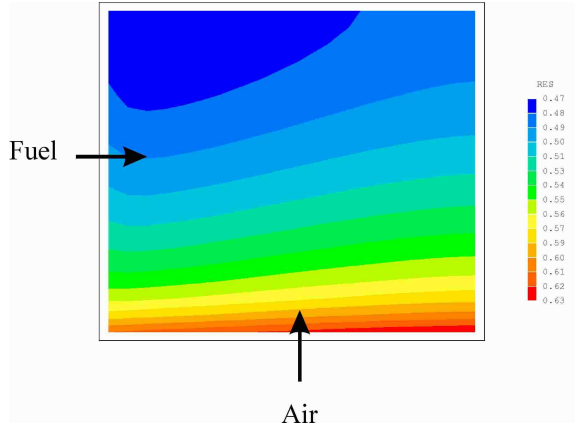
Figure 5. Nernst potential, E, $\bar{i}$ = 4 000 A/m^2

Figure 6. Lumped resistance, r_l, $\bar{i}$ = 4 000 A/m^2

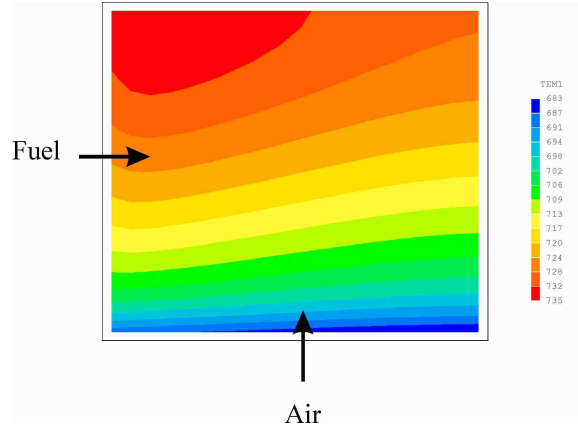Figure 7. Temperature, T (°C), $\bar{i}$ = 4 000 A/m^2
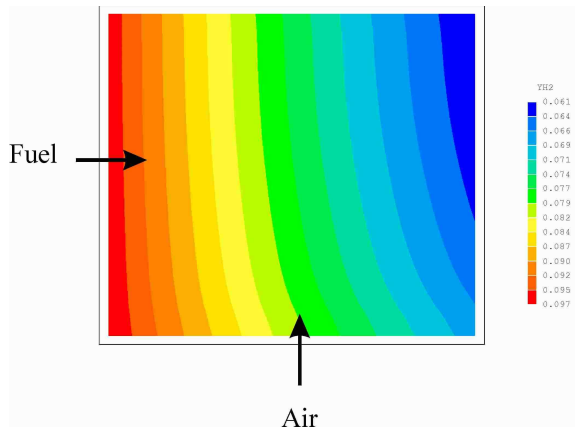

Figure 8. Anodic H_2 mass fraction, $\bar{i}$ = 4 000 A/m^2
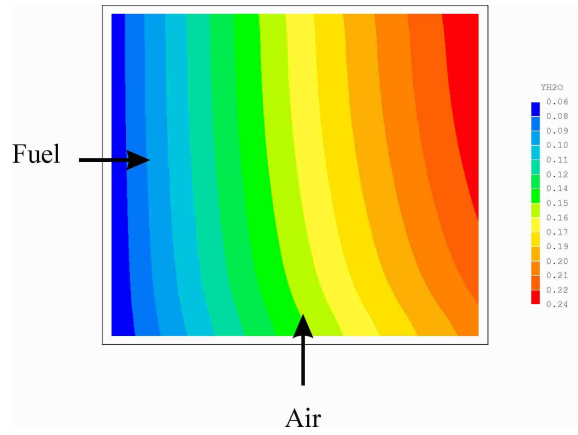
Figure 9. Anodic H_2O mass fraction, $\bar{i}$ = 4 000 A/m^2

YO2
0.18
0.18
0.19
0.19
0.19
0.20
0.20
0.20
0.21
0.21
0.21
0.21
0.22
0.22
0.22
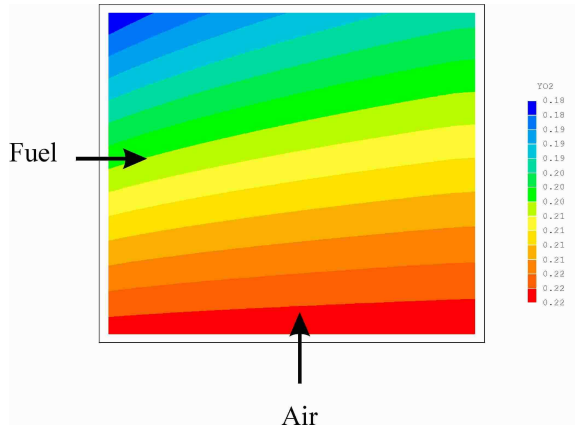
Figure 10. Cathodic O_2 mass fraction, $\bar{i} = 4\ 000$ A/m^2

POW
2417
2551
2685
2819
2953
3087
3220
3354
3488
3622
3756
3890
4024
4158
4292

Figure 11. Power density (W/m^2°C), $\bar{i} = 4\ 000$ A/m^2

Figure 12. Temperature distribution in a SOFC using detailed CFD simulation. Current density and cell resistance presumed constant

Figure 13. Temperature distribution in air space of SOFC stack, using a MUSES approach. Current density and cell resistance presumed constant.

RESULTS AND DISCUSSION

Figures 4 to 11 show results for $\bar{i}$ = 4 000 A/m^2, based on the detailed model. Figure 4 shows the current density, Fig. 5 o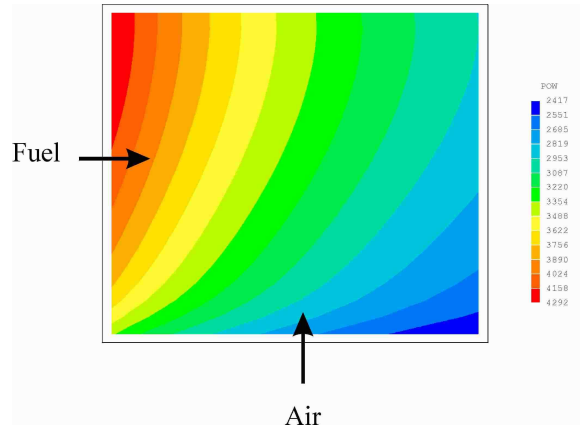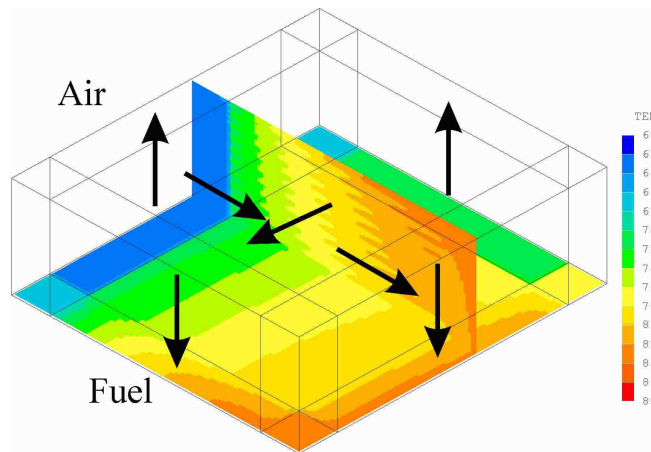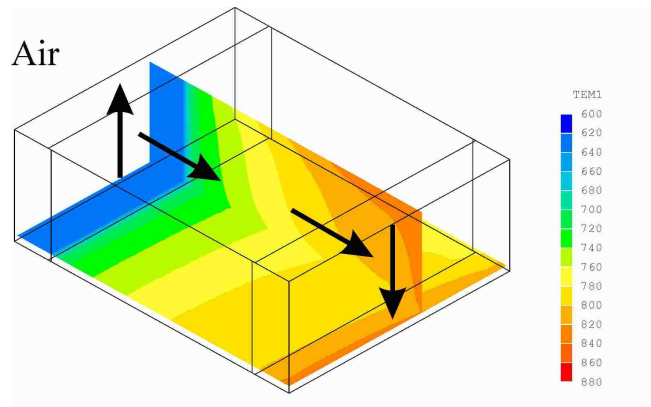pen-circuit voltage, Fig. 6 lumped resistance, Fig. 7 temperature. The mass fractions, y_{H2}, y_{H2O}, y_{O2} , are exhibited in Figs. 8-10. Fig. 11 shows power density for this case

The open-circuit-voltage was found to be essentially independent of cell voltage, while the mean current density is inversely proportional to cell voltage. Fuel utilisation decreases as a function of *V*. Since the contact area is almost double for case (a) than for case (b), the fuel utilisation is larger. In order to maximise fuel utilisation, cell voltage must be decreased; conversely at practical cell voltages, the fuel utilisation may be compromised. The problem may be considered as a trade-off between optimising fuel utilisation and cell voltage: In practical fuel cell design local flow distribution impacts on fuel utilisation, and hence overall performance.

The pressure distribution in both fluids (not shown) is quite uniform throughout stack; in spite of flow variations in the inlet manifolds. This is because, as discussed in Beale et al. (2000), if pressure losses across the manifolds are small compared to those across the stack, the flow and pressure distributions will be quite uniform within the core of the stack. The MUSES method breaks up the interpenetrating continua into three (or more) domains facilitating graphical analysis readily.

Figures 12-13 show the temperature distributions in a stack: Horizontal and vertical planes are shown. Variations in the vertical direction (i.e. 3-D) effects are apparent in Fig. 12. These will have an impact on reaction rates, although they are less significant than the primary gradients in the stream-wise plane which, as already discussed are always present due to Ohmic heating, regardless of the spatial distribution of the local current density. The 'zig-zag' profile arises because the air and fuel (and electrolyte and interconnect) are at substantially different temperature. These are only apparent in detailed numerical simulations; local volume averaging removes these perturbations entirely, although the temperature differences are reflected in the different spaces. It is noted that the MUSES-based distributed resistance analogy method was modified, as discussed in Beale et al. (2002) in order to generate the 3-D temperature fields shown in Fig. 13. This involves 'breaking the link' for the electrode-fuel pair of inter-phase source terms so that these terms were prescibed to (north-south) neighbours rather than in-cell values at *P*. With this important modification, it can be seen that this approach closely mimics the results for a detailed CFD simulation at a fraction of the computational cost.

Because the flow is laminar; detailed numerical simulations can be relied upon to produce very accurate predictions of the performance of SOFC's. However the computational overhead is very large. While in the future such calculations may be routine, at present these computational resources are significant by any standards, i.e. they could not be entertained on a day-to-day operation by fuel cell engineers not familiar in computational fluid dynamics. Moreover visualizing and analyzing the results of these data sets is far from easy due to the multiplicity of intermingling continua; display and manipulation of pressure and velocity data is far from easy.

Distributed resistance methods still require significant compute times, though not the same magnitude as are required for detailed simulations. It is true that some of the finer details are inevitably lost, however the approach allows for a reasonably accurate solution to be obtained in a reasonably short time. An advantage of the technique used in this paper is that diffusive effects may be included/excluded in different zones, so that a rate equation can be used selectively in certain regions, such as the stack core, but not in other regions such as manifolds and solids, where viscous and conduction terms are computed directly. The technique also allows for as many inter-phase terms (fluid-fluid, fluid-wall) etc. to be introduced as required.

In the distributed resistance method, the overall heat transfer coefficients as well as the wall mass fractions are computed from an appropriate Nusselt/Sherwood number correlation. Thus the reliability of the calculations will depend on the efficacy of the appropriate correlations. In this study we used values (Kays and Crawford, 1966) appropriate for constant flux (Neumann), rather than constant value (Dirichlet), however neither of these are strictly correct. Alternatively these may be obtained from experimental or detailed numerical analyses for the same design.

The distributed resistance analogy was originally developed to model transport phenomena in shell-and-tube heat exchangers, where there are substantial variations in the gross motion due to the presence of baffles. For the equipment under consideration; because the passages are straight and narrow, the flow is essentially uniform (notwithstanding mass sources/sinks due to the chemical reactions). Thus the computational overhead associated with the distributed resistance analogy is barely justified; since inertial effects are very small for the particular geometry under consideration. Coupling the presumed-flow heat/mass transfer solution for the fuel-cell stack to a flow

solution for the manifolds etc. would appear to offer all the advantages of the distributed resistance analogy approach, with potential benefits in terms of speed of convergence, discussed below.

CONCLUSIONS AND FUTURE WORK

PHOENICS has been used to develop SOFC models in which calculations for fluid flow, heat and mass transfer, with electrochemistry are performed. The current models are still undergoing development but it is maintained that the models are robust enough to be used for the purpose of design and performance prediction of SOFC's. Detailed numerical simulations provide the best possible alternative to gathering of experimental data however they are very time-consuming and expensive. An alternative method is the distributed resistance analogy which offers the potential for both speed and the ability to compute complex 3D flows accurately. Further model development for SOFC's is ongoing. and all the models will be validated against each other and, when available, detailed experimental work.

ACKNOWLEDGEMENTS

REFERENCES

Achenbach E. Three-dimensional modelling and time – dependent simulation of a planar solid oxide fuel cell stack. J. Power Sources. Vol.73, pp:333-348, 1994

Appleby, A.J., and Foulkes, F.R. *Fuel Cell Handbook*, Van Nostrand Reinhold, New York, 1989

Archer D.H., and Sverdrop E.F. Solid electrolyte barriers. Proc. 18th Annual Power Sources Conference. 1962

Beale, S.B., Ginolin, A., Jerome, R., Perry, M., Ghosh, D. Proc. 8th Conference CFD Soc. Canada, 2000, Vol.1, pp. 489-494

Beale, S.B., S.V. Zhubrin, S.V., Dong, W. Numerical Studies of of Solid-oxide Fuel Cells, Proceedings 12th International Heat Transfer Conference, Grenoble, France 2002, pp. 865-870.

Bessete N.F., and Wepfer W.J. A mathematical model of a tubular solid oxide fuel cell. J. Energy Resources Technology. Vol.117, pp.43-49. 1995

Boersma R.J., and Sammes, N.M. Distribution of Gas Flow in Internally Manifolded Solid Oxide Fuel-Cell Stacks. J. Power Sources, Volume 66, pp.41-45, 1997

Ding J., Patel P., Farooque M., and Maru H.C. A computer model for direct carbonate fuel cells. Proc. 4th Int. Symp. on Carbonate Fuel Cell Technology, Proc. Vol.97-4, pp:17-138. 1997

Dunbar W.R., Lior N., and Gaggioli R. A. (1990). The exergetic advantages of fuel cell system. Proc. Florence World Energy Research Symposium, UK.

Foster R.E. Computer modelling of a novel tubular SOFC concept. Electrochem. Soc. Proc. Vol.99-19, 1999

Ghosh D., Wang G, Brule R, Tang, E. and Huang P. Performance of anode supported planar SOFC cells. Unpublished, 2001

He W., and Chen Q. Three-dimensional simulation of a molten carbonate fuel cell stack under transient conditions. J. Power Sources. Vol.73, pp:182-192. 1998

Kays, W.M. and Crawford, M.E. *Convective Heat and Mass Transfer,* 2nd ed., McGraw-Hill, New York, 1966

Mueller, A.C. Heat Exchangers. in Rohsenhow, W.M., Hartnett, J. *Editors*. *Handbook of Heat Transfer.* McGraw-Hill, Chapter 18, 1973

Patankar S.V. Numerical heat transfer and fluid flow. Taylor and Francis, Hemisphere, New York, 1980

Patankar, S.V., and Spalding, D.B. TR EF/TN/A/48, Imperial College, London, 1972

Sverdrup E.F., Warde C.J., and Eback R.L. Design of high temperature solid-electrolyte fuel–cell batteries for maximum power output per unit volume. Energy Conversion Management. Vol.13, pp:129-136. 1973

Wepfer W.J., and Woolsey M.H. High temperature fuel cells for power generation. Energy Conversion Management. Vol.25, pp:477-485. 1984

Yakabe H., Ogiwara T., Yasuda I., and Hishinuma M. Model calculation for planar SOFC focusing on internal stresses. Electrochem. Soc. Proc. Vol.99-19, 1999